INTERNATIONAL JOURNAL OF HYDROGEN ENERGY 39 (2014) 8767–8771

Available online at www.sciencedirect.com

ScienceDirect

journal homepage: www.elsevier.com/locate/he

Formation kinetics and microstructure of Mg–Ti hydrides made by reactive ball milling

A. Biasetti*, M. Meyer, L. Mendoza Zélis

IFLP, Departamento de Física, Facultad Ciencias Exactas, Universidad Nacional de La Plata, 1900 La Plata, Argentina

ARTICLE INFO

Article history:
Received 31 October 2013
Accepted 4 December 2013
Available online 18 January 2014

Keywords:
Hydrogen storage
Reactive milling
Nanocomposites

ABSTRACT

In this work we report the formation kinetics and microstructural properties of $Mg_{1-x}Ti_x$ powder metal hydride systems ($x = 0.1, 0.2, 0.3, 0.4, 0.5$), obtained by reactive ball milling (RBM) via three different ways. The resulting MgH_2–TiH_2 nanocomposites are characterized and an optimal composition is found. Differences among the preparation routes are analyzed.

1. Introduction

Magnesium and magnesium alloy hydrides have been investigated as hydrogen storage materials because of their relevant properties such as high hydrogen capacity, availability and low cost. The need to improve the kinetic properties of such systems, in order to convert them in promising materials for hydrogen storage, lead to the search for catalysts of the $Mg + H_2 \leftrightarrow MgH_2$ reversible reaction [1].

Recently, some progress was made in the field, fabricating MgH_2–TiH_2 nanocomposites by milling Mg–Ti mixtures under a relatively high (8 MPa) H_2 pressure [2]. Practical conditions are required for a hydrogen storage system to be considered useful as such. Although we are exploring the formation properties of that systems as potential reservoirs, the same demand must be kept for their fabrication too. With this aim we start an investigation to explore the formation of such MgH_2–TiH_2 nanocomposites by milling at low H_2 pressure (less than 0.3 MPa) and starting from different primary materials.

The studied samples consisted of heterogeneous systems which were prepared from Mg–Ti powder mixtures with different Mg:Ti ratios, mechanically ground in H_2, obtaining fine dispersions of MgH_2 and TiH_2 phases. Preparation has been performed following three different routes, all of them consisting in the milling of the powder mixture with certain Mg:Ti ratio under H_2 atmosphere, but varying in each method the accomplishment or not of a pre-milling treatment.

A pressure sensor let the hydrogen consumption to be measured as the grinding is performed and then kinetic curves were obtained for the hydride formation reactions as a function of the milling time. Both the kinetic curves and their corresponding derivatives, support the idea of the existence of well separated formation stages for MgH_2 and TiH_2. Therefore we have proposed a mixed function, built up from the sum of two sigmoidal type functions, in order to fit the experimental kinetic curves.

The resulting phases were identified by X-ray diffraction (XRD), technique which also yields an estimation of grain sizes and microstrain. In a second stage of our research the

* *Corresponding author*. Tel.: +54 221156723322.
E-mail address: abiasetti@exactas.unlp.edu.ar (A. Biasetti).
0360-3199/$ – see front matter
http://dx.doi.org/10.1016/j.ijhydene.2013.12.034

hydrogen sorption properties under thermal activation will be investigated.

2. Experimental

The mixtures obtained from Mg granules and Ti powder, both of high purity (99.9% and 99.4% respectively), were ground in a vibratory ball mill (modified Retsch MM2) in H_2 atmosphere at a starting pressure of 280 kPa. The Mg:Ti ratios considered were 50:50, 60:40, 70:30, 80:20 and 90:10. A ball to sample mass ratio of about 15 and a grinding frequency of 32 Hz were used. Employing a gauge transducer (0.5 kPa of sensibility) the pressure in the reaction chamber was recorded during the process. When the pressure fell below 220 kPa because of the hydrogen absorption by the metals, the gas was injected automatically restoring the initial value of pressure. The system then kept the pressure bound in the range 220–280 kPa. Kinetics curves were built up from this information, reconstructing the curve of hydrogen consumption [3].

The mentioned three routes of preparation of the systems were the following:

a) Milling directly under H_2 atmosphere powders mixtures of Mg and Ti in the proportions mentioned above;
b) Similar mixtures were previously milled in Ar atmosphere and later under H_2 atmosphere;
c) Milling under H_2 atmosphere powder mixtures of Mg and TiH_2 (obtained previously by similar method), in the adequate proportions.

Diffraction patterns were obtained by using Cu Kα radiation with a Philips PW1710 difractometer. Bragg geometry was used, in the range 2θ: 20°–80°, with steps of 0.05°. For selected samples ($Mg_{80}Ti_{20}$) a step of 0.02° were used to improve the statistics in order to perform a Rietveld refinement.

3. Results

The progress in the absorption reactions during reactive ball milling was obtained considering the instantaneous fraction $f(t)$ of hydrogen atoms incorporated to the mixture relative to the number of metallic atoms. This is calculated from

$$N_H(t) = -\Delta P(t)V/RT \text{ and } N_M = N_{Mg} + N_{Ti}.$$

The formation kinetic curves are shown in Fig. 1. Emphasis has been placed on the compositional evolution of kinetics, which appears to be strongly dependent on the Mg:Ti ratio. The hydrogen capacity resulted in a value $f(t\rightarrow\infty)\approx f_{máx} = 2,0$ for all the samples obtained by direct milling (route *a*). Comparing the three preparation methods presented in Fig. 1, it can be seen that the reaction $Mg \rightarrow MgH_2$ can be considered almost complete for routes *a* and *c*. Instead for route *b* the reaction is clearly not complete.

In the diffraction patterns for all fabrication routes, phases γ-MgH_2 (metastable) [4], rutile-MgH_2 and δ-TiH_2 have been identified. It is worth to note that the ε-TiH_2 phase results indistinguishable from the δ one in the present data. A small

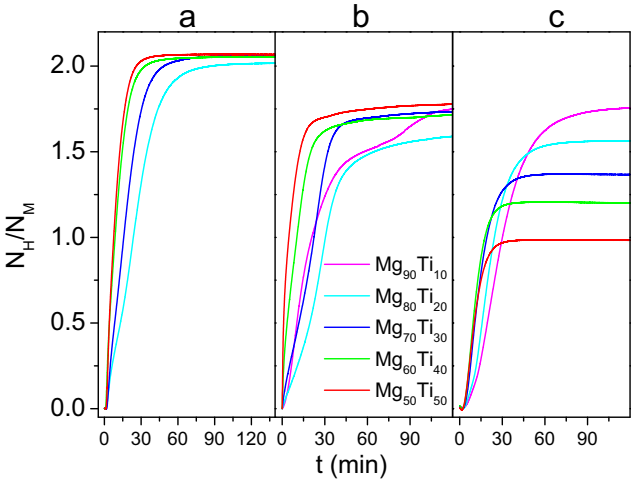

Fig. 1 – Formation kinetic curves for all the studied compositions prepared by: a) route *a*; b) route *b*; c) route *c*.

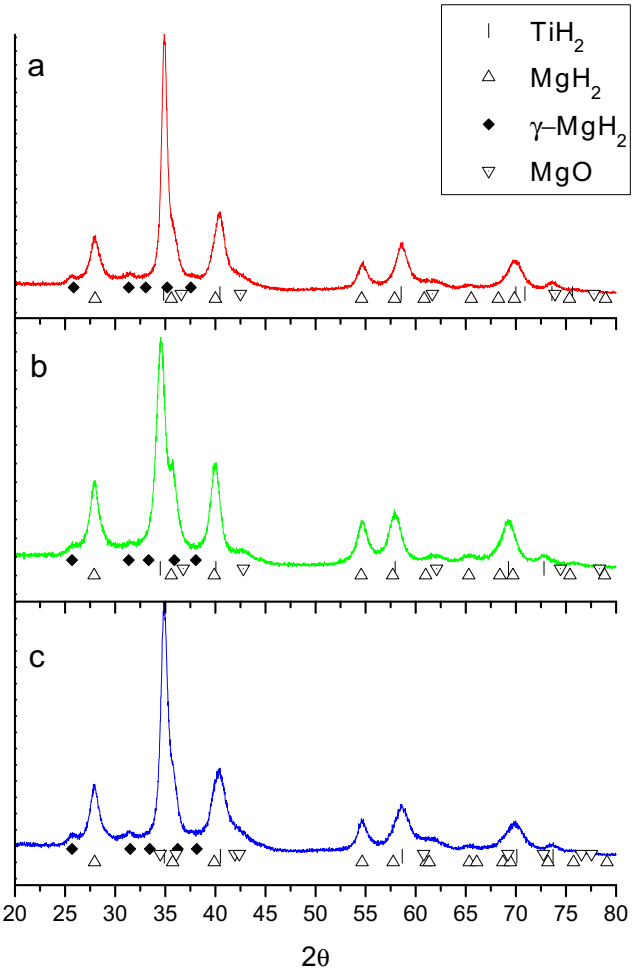

Fig. 2 – XRD patterns for 80:20 composition samples prepared by: a) route *a*; b) route *b*; c) route *c*. Also shown are the peak positions for the main phases observed.

proportion of MgO had also to be considered to improve the fit quality. Oxidation was unavoidable during XRD measurements performed at open atmosphere. The XRD patterns of $Mg_{80}Ti_{20}$ are reported in Fig. 2, where a change in the cell dimensions of TiH_2 phase for milling route *b* is evident.

4. Analysis and discussion

4.1. Capacity and kinetics

Generally the formation kinetics curves have a sigmoidal growing form. This behaviour is described by the differential equation $y'(t) = k(t)\cdot y(t)$ where $k(t)$ is the instantaneous growth rate, and is related to the number of atoms able to absorb hydrogen. In our particular case the number of atoms capable to absorb hydrogen must reduce with time, because formation of hydride phase implies reduction of metallic ones. Further, $k(t)$ must tend to zero for increasing times. Models with $k(t) = a\cdot t^{-n}$ did not lead to good fits to the experimental data. Instead, reasonable fits were obtained if an exponential decay is assumed for $k(t)$. This model leads to the so called Gompertz function $y(t) = ae^{-e^{-b(t-c)}}$ as the general solution.

To model the observed two stage behaviour, we adopt this functional form for each of the process identified in our kinetic curves, thus we have a kinetic curve consisting of a sum of two Gompertz functions, each one representing the different stages.

$$y_S(t) = y_1 + y_2 = a_1 e^{-e^{-k_1(t-tm_1)}} + a_2 e^{-e^{-k_2(t-tm_2)}}$$

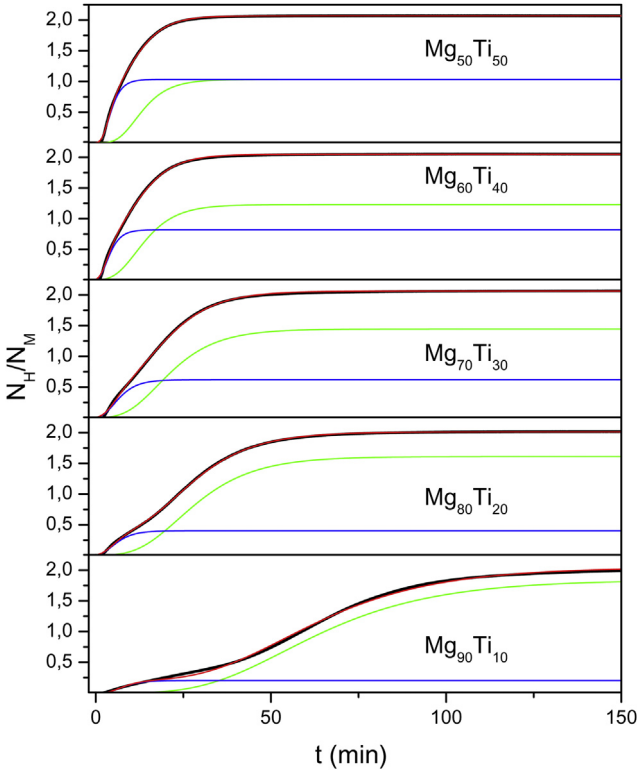

Fig. 3 – Kinetic curves for samples obtained by route *a* fitted with the proposed sum of two Gompertz functions.

Table 1 – Fitted parameters for the kinetic curves of hydrides made by route *a* and *c* with different Mg:Ti ratio, using the function described in the text. Index 1 and 2 correspond respectively to the formation of MgH_2 and TiH_2.

Mg:Ti ratio	Kinetic parameters		
	Route *a*		Route *c*
90:10	a_1: 1.84	a_2: 0.20	a_1: 1.7589(6)
	k_1: 0.0426(2)	k_2: 0.13(2)	k_1: 0.0721(2)
	t_{m1}: 53.9(1)	t_{m2}: 4.9(6)	t_{m1}: 22.65(4)
80:20	a_1: 1.6	a_2: 0.4	a_1: 1.560(3)
	k_1: 4.5276	k_2: 5.4214	k_1: 0.1060(2)
	t_{m1}: 23.58(2)	t_{m2}: 4.63(2)	t_{m1}: 16.97(2)
70:30	a_1: 1.44	a_2: 0.6	a_1: 1.3665(4)
	k_1: 0.195(6)	k_2: 0.286(6)	k_1: 0.1470(6)
	t_{m1}: 17.75(5)	t_{m2}: 5.25(5)	t_{m1}: 11.10(2)
60:40	a_1: 1.23	a_2: 0.8	a_1: 1.2001(2)
	k_1: 0.162(1)	k_2: 0.461(7)	k_1: 0.1986(7)
	t_{m1}: 11.47(4)	t_{m2}: 3.14(2)	t_{m1}: 11.10(2)
50:50	a_1: 1.033	a_2: 1.033	a_1: 0.9821(2)
	k_1: 0.193(1)	k_2: 0.489(5)	k_1: 0.2025(7)
	t_{m1}: 11.34(3)	t_{m2}: 3.64(1)	t_{m1}: 8.43(1)

For the fits to be consistent with the stoichiometric proportion given in each system we must fix the constrains $a_1 + a_2 = f_{máx}$, $a_1 = f_H(TiH_2)$, $a_2 = f_H(MgH_2)$.

It is clear that just one component should be sufficient to fit the corresponding kinetic curves for the samples made by route *c* with the Ti fraction already as TiH_2. The resulting fits are presented in Fig. 3 and the fitted parameters are reported in Table 1.

To have a better knowledge of the transformation process rates, the derivatives of the original formation kinetic curves, were built. Those are presented in Fig. 4. In the case of direct method, all derivatives have a two maxima structure suggesting the existence of two more or less distinguishable stages for the reacted fraction. We associate the first maximum with the formation process of TiH_2 because of its lower enthalpy respect to MgH_2 formation, which in turn can be associated with the second maximum.

In order to have a characterization of kinetic properties we may define a characteristic time t_m as that corresponding to the maximum transformation velocity. The resulting values are quoted in Table 1 and show a notorious reduction in characteristic times with increasing Ti.

4.2. XRD-phases, strain and grain size

The Powder cell code was used to fit the structure of each single phase to the experimental data. The identification of only hydride phases does agree with the completeness of reactions $Mg \rightarrow MgH_2$ and $Ti \rightarrow TiH_2$. As mentioned before MgO is produced during XRD measurements performed at open atmosphere. Fig. 5 shows the results for one sample obtained by route *a*.

The FWHM of each of the single phase peaks, were obtained from those fits. For the samples fabricated via routes *a* and *c*, the Scherrer model indicates a decreasing grain size for the rutile-MgH_2 with the increase in the Ti proportion of the mixture. This can be assigned to the abrasive properties of TiH_2 which is formed in a first stage [1].

Table 2 – Parameters obtained from the refinement of XRD patterns of samples with 80:20 composition and different fabrication routes. L is the average grain size.

Method	Phase	Cell parameters [nm]			L [nm]	Content [wt%]
a	β-MgH_2	*a*: 0.45013		*c* 0.30435	6.54	42.79
	γ-MgH_2	*a*: 0.44528	*b*: 0.54204	*c*: 0.51	12.68	6.37
	δ-TiH_2	*a*: 0.4456			17.1	40.10
	MgO	*a*: 0.425			5.68	10.74
b	β-MgH_2	*a*: 0.45159		*c*: 0.3035	8.2	48.07
	γ-MgH_2	*a*: 0.4606	*b*: 0.53756	*c*: 0.499	6.18	6.88
	δ-TiH_2	*a*: 0.4581			9.75	37.86
	MgO	*a*: 4.25			12.54	7.2
c	β-MgH_2	*a*: 0.4513		*c*: 0.302	8.5	45.98
	γ-MgH_2	*a*: 0.4537	*b*: 0.5356	*c*: 0.4954	7.0	7.01
	δ-TiH_2	*a*: 0.4446			14	27.38
	MgO	*a*: 4.306			3	19.8

A Williamson–Hall analysis of the peaks width for the 80:20 samples yields grain sizes similar to those obtained by the Scherrer method and microstrain values typical of mechanically alloyed samples. An increase in the lattice constant for the TiH_2 phase in the sample obtained by route *b* may be attributed to some Mg dilution in the TiH_2 lattice.

A Lorentzian line profile function was needed for the structure fit of all phases in each one of the prepared systems, with the exception of TiH_2 which required a pseudovoigt profile function in the samples fabricated though the route *c*.

Concerning the metastable γ-MgH_2 phase, it is found usually in ball milled Mg hydrides and does not affect the hydrogen capacity of the system. Furthermore, we expect that it would convert into the stable rutile-MgH_2 under thermally activated hydrogen release and uptake processes.

5. Conclusions

A remarkable enhancement in the formation kinetics was found with the increment of Ti proportion in $Mg_{1-x}Ti_x$ systems. Making a balance between the need for fast kinetics and undesirable low gravimetric density, one can establish that compositions around $x = 0.2–0.3$ have the better properties without appreciable loss of hydrogen capacity. In particular for route *c*, the MgH_2 formation rate does not increase further for $x \geq 0.4$, setting $x = 0.3$ as an optimal composition.

On the other hand, satisfactory fits with the model of two Gompertz components are in agreement with the identification of the separated formation stages for TiH_2 and MgH_2 in the case of route *a*. That is why a unique component fits well the kinetic curves for the route *b* in which the TiH_2 is already prepared when the milling starts. Therefore the parameters k_i can be interpreted as kinetic constants characterizing both processes.

The greater reaction velocities correspond to route *c* and this denotes the catalytic role played by TiH_2. This route would then constitute a possible way for the fabrication of a hydrogen reservoirs with a stable TiH_2 phase as a catalyst for the complete reaction $Mg \rightarrow MgH_2$.

In summary, we have confirmed the adequacy of the ball milling under low H_2 pressure to prepare this kind of MgH_2–TiH_2 nanocomposites, starting from different primary materials. This encourages further studies on the kinetics of H_2 thermal sorption of these systems and their stability under repeated cycles of hydrogen uptake and release.

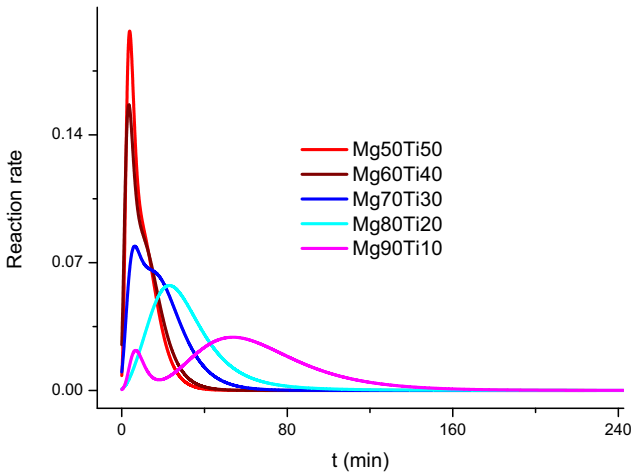

Fig. 4 – Derivatives of the kinetic curves shown in Fig. 3.

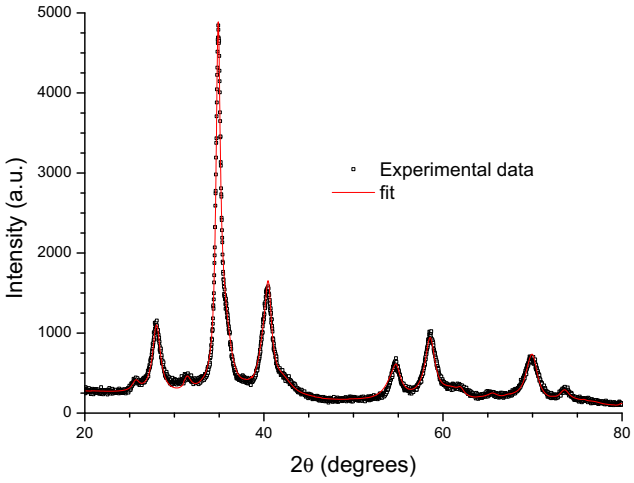

Fig. 5 – XRD pattern for 80:20 composition samples made by route *a* and the corresponding refinement yielding the parameters quoted in Table 2.

REFERENCES

[1] Selvam P, Viswanathan B, Swamy CS, Srinivasan V. Magnesium and magnesium alloy hydrides. Int J Hydrogen Energy 1986;11:169–92.

[2] Cuevas F, Korablov D, Latroche M. Synthesis, structural and hydrogenation properties of Mg-rich MgH_2–TiH_2 nanocomposites prepared by reactive milling under hydrogen gas. Phys Chem Chem Phys 2012;14:1200–11.

[3] Meyer M, Mendoza Zélis L, Baum L. Complex quaternary hydrides Mg_2(Fe, Co)H_y for hydrogen storage. Int J Hydrogen Energy 2011;36:600–5.

[4] Bortz M, Bertheville B, Böttger, Yvon K. Structure of the high pressure phase γ-MgH_2 by neutron powder diffraction. J Alloy Compd 1999;287:L4–6.